Optica Applicata, Vol. LI, No. 1, 2021
DOI: 10.37190/oa210107

Wide-angle infrared plasmonic perfect absorber based on graphene-silica grating

FANG CHEN

Institute of Quantum Optics and Information Photonics,
School of Physics and Optoelectronic Engineering, Yangtze University,
Jingzhou 434023, People's Republic of China;
chenfang@yangtzeu.edu.cn

In this paper, wide-angle infrared perfect absorption has been demonstrated by using a double-layer graphene strip grating coupled with a silicon dioxide grating. Numerical simulation of the finite-difference time-domain method indicates that the perfect absorption can be achieved due to the effective impedance matching, and all the incident electromagnetic energy is confined in the Al_2O_3 layer between the silver substrate and the graphene strip grating. Dual-band perfect absorption is achieved with the change of strip width or chemical potential of the bi-layer graphene strip grating. It is found that the spectral position of the absorption peak can be tuned by the chemical potential or the width of the graphene strip, and additionally by the size of the proposed absorber. Moreover, the proposed perfect absorber shows excellent absorption stability for a wide range of the incident angle up to ±65°. The proposed absorber may find potential application in tunable double band perfect absorbers in the mid-infrared range.

Keywords: plasmonic resonance, graphene grating, optical absorption, plasmonic absorber.

1. Introduction

Graphene is a two dimensional carbon crystal with a honeycomb lattice, which attracted a lot of attention because of its outstanding optical properties like surface conductivity, high mean free path, high mobility and low switching time as 10^{-13} s [1–3]. The main excellent point is that graphene material is easily tunable by chemical doping or electrical gating, which makes graphene an excellent optical material in designing plasmonic devices, such as plasmonic tunable absorbers [4–6], plasmonic filters [7, 8], graphene photodetectors [9], sensors and many other electronic devices [10].

In recent years, metamaterials and metasurfaces composed of periodic graphene structures have been investigated theoretically and demonstrated experimentally. Metamaterials have a lot of exotic characteristics, such as negative index, plasmonic perfect absorber, invisibility cloaking and transformation optics [6, 11–13]. For a plasmonic absorber, many narrow band or wide band, angle dependent, polarization independent plasmonic absorbers have been studied in the visible, infrared or terahertz range. For example, in 2016, LU *et al*. investigated tunable high efficiency light absorption in

a graphene coupled multilayer photonic structure [14]. One year later, LU *et al*. numerically studied perfect absorption in monolayer molybdenum disulfide (MoS_2) [15]. LI *et al*. proposed and studied multiband plasmonic metamaterial perfect absorbers based on graphene ribbons by the phase coupled method [16]. LI *et al*. also numerically demonstrated a tunable graphene-based mid-infrared plasmonic wide-angle narrow band perfect absorber [17]. Very recently, our group reported a tunable plasmonic perfect absorber based on the multilayer graphene strip grating structure [18]. Graphene based perfect plasmonic absorbers can be actively tuned by means of the external gate voltage technology instead of refabricating a new structure by changing the geometrical sizes. Therefore, utilizing external gate volatge of graphene material, electrically controlled tunable plasmonic devices based on graphene material can be realized.

Inspired by earlier works [19–21], this paper combines the graphene strip with the dielectric grating structure, and a wide angle plasmonic perfect absorber based on the periodic bi-layer graphene strip separated by Al_2O_3 layer is studied theoretically. The perfect absorption can be attributed to the impedance matching, the position of an absorption peak and the absorptance can be tuned by changing geometrical sizes or chemical potential. Moreover, by controlling the chemical or the graphene strip width, a double band perfect absorber can be obtained. The designed graphene-based absorber has an excellent absorption stability over a wide angle range of incidence around ±65°. The results of this paper may have potential applications in plasmonic sensors, optical storage and plasmonic sensors in the mid-infrared range [22–25].

2. Geometry and simulation method

The proposed plasmonic perfect absorber is schematically depicted in Fig. 1**a**, which consists of a bi-layer graphene strip grating, SiO_2 grating, Al_2O_3 dielectric layer and a silver substrate. The unit cell of the side view of the proposed periodic structure is shown in Fig. 1**b**, and the geometrical parameters are as follows: the thickness of SiO_2 grating, Al_2O_3 layer and silver substrate are t_1, t_2 and t_3, respectively. The period and width of

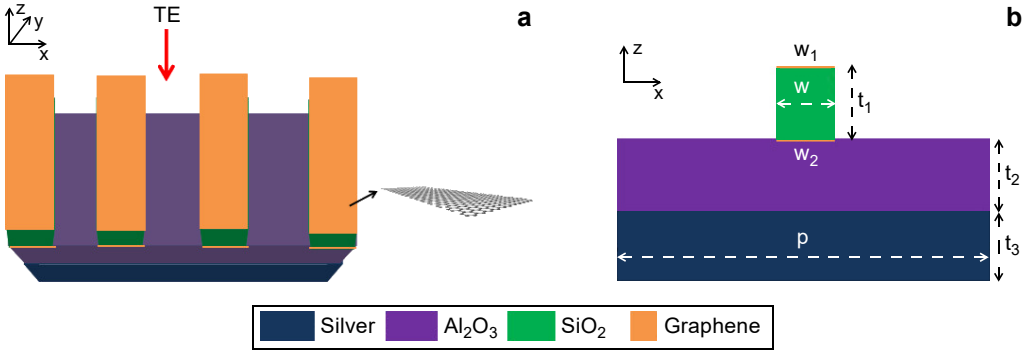

Fig. 1. Schematic of the proposed graphene-SiO_2 grating-based plasmonic absorber, the complex grating is on the Al_2O_3 layer and a silver substrate (**a**). The *x*-*z* cross-section of a unit cell of the proposed plasmonic absorber (**b**).

SiO_2 grating are p and w, respectively. The widths of the upper and lower graphene strip are denoted by w_1 and w_2, respectively. In the numerical calculation, the graphene strip is modeled as an ultra-thin film with a thickness of 1 nm in the z direction. Due to the periodicity of the proposed structure, the simulation domain is made up of a single unit of the structure with periodic boundary conditions which are imposed in the x and y direction, while in the z direction, a perfectly matched absorption boundary condition is used. A plane wave source with polarization along the x direction is normally incident from the z direction. In order to further reduce the simulation time, the simulation length along the y direction is chosen to be 5 nm with periodic boundary conditions, and the total simulation area is 300 nm × 5 nm × 300 nm. With the transmittance T and reflectance R obtained from finite-difference time-domain (FDTD) method, the absorption A of the plasmonic absorber can be calculated by the relationship $A = 1 - T - R$. In the proposed structure, the metal substrate is 400 nm, which is thick enough so the transmission can be approximately regarded as zero, therefore the absorption A can be calculated by $A = 1 - R$.

Graphene is a special two-dimensional gapless carbon material, which is determined by the well-established and experimentally valid theoretical model. The complex surface conductivity can be calculated from Kubo's formula [26]:

$$\sigma_{S,G}(\omega, \Gamma, \mu_c, T) = \sigma_{inter}(\omega, \Gamma, \mu_c, T) + \sigma_{intra}(\omega, \Gamma, \mu_c, T) \tag{1}$$

where $\sigma_{inter}(\omega, \Gamma, \mu_c, T)$ and $\sigma_{intra}(\omega, \Gamma, \mu_c, T)$ stand for the absorption corresponding to the interband electron transition and intraband electron photon scattering, respectively. Further, the permittivity of the graphene is defined as:

$$\varepsilon_{V,G}(\omega) = 1 + j\frac{\sigma_{S,G}(\omega)}{\varepsilon_0 \omega \delta} \tag{2}$$

where δ is the thickness of the graphene strip, ε_0 is the free space permittivity. In the following FDTD simulation, the parameters of the graphene are set as: $T = 300$ K, $\Gamma = 0.658$ meV, and $\delta = 1$ nm. The permittivity of the Al_2O_3 layer and SiO_2 grating are set to 1.76 and 1.45, respectively. The metal in the proposed paper is silver whose frequency-dependent complex permittivity is described by the Drude model.

Figure 2 shows the absorption spectra with $p = 300$ nm, $w = w_1 = w_2 = 150$ nm, $t_1 = 200$ nm, $t_2 = 800$ nm, $t_3 = 400$ nm, and $\mu_{c1} = \mu_{c2} = 0.6$ eV. The perfect absorption peaks occurs at 13.07 μm, the FWHM of the absorption peak is about 310 nm. To investigate the origins of the perfect absorption effect, we examined the steady state field E_z, and $|H_y|$ distributions of the unit cell. Figure 3 shows the steady state electric field E_z distributions of the proposed bi-layer graphene-SiO_2 grating at the resonant wavelength 13.07 μm. It can be noticed that a dipole resonance occurs and electric field distributions occur around the edges of the graphene strip, and the near-field coupling between the two graphene strips is weak due to a larger coupling distance. The magnetic field $|H_y|$ distributions of the proposed bi-layer graphene-SiO_2 grating at the resonant wavelength 13.07 μm and the nonresonant wavelength 15 μm are also shown in Fig. 3.

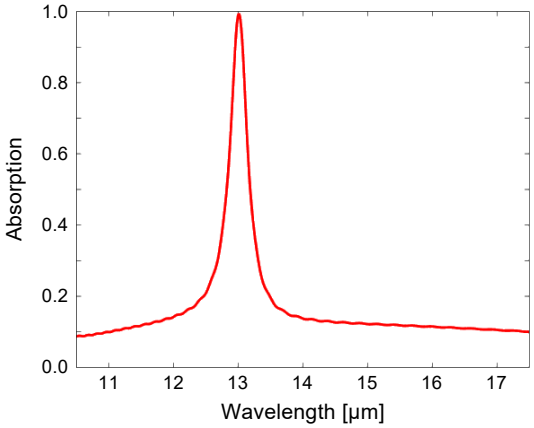

Fig. 2. Absorption spectra of the proposed absorber. The period and width of the graphene strip and SiO_2 grating are $p = 300$ nm, $w = 150$ nm and $w_1 = w_2 = 150$ nm. The thickness of SiO_2 grating, Al_2O_3 layer and silver substrate are $t_1 = 200$ nm, $t_2 = 800$ nm, and $t_3 = 400$ nm, respectively. The chemical potential of the graphene is $\mu_{c1} = \mu_{c2} = 0.6$ eV.

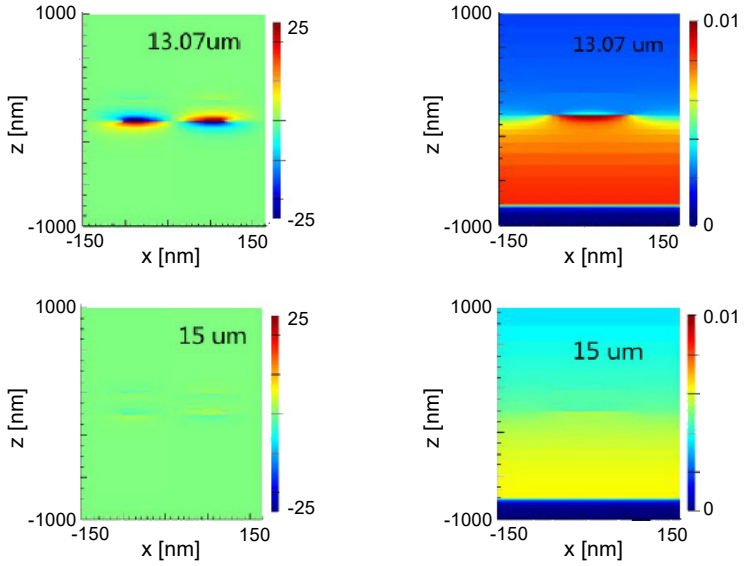

Fig. 3. Electric field E_z and magnetic field $|H_y|$ distributions of the unit cell graphene-SiO_2 grating at the resonant wavelength of $\lambda_0 = 13070$ nm, at nonresonant wavelength $\lambda = 15000$ nm.

It can be noticed that at the resonant wavelength 13.07 μm, since the effective impedance (EI) of the bi-layer graphene-SiO_2 grating is equal to that of the free space, the reflection is suppressed and all the input energy is confined in the Al_2O_3 layer. The perfect absorption occurred by the proposed hybrid structure, while at the nonresonant wavelength 15 μm, the EI of the proposed absorber mismatched to the free space, and the incident energy could not be confined in the Al_2O_3 layer.

Since the position of the absorption peak is related to the dipole resonance of the graphene strip, the natural resonant wavelength of the graphene strip is determined by the strip width and chemical potential [27]:

$$\lambda = \frac{\pi c}{0.31}\sqrt{\frac{n^2\hbar^2\varepsilon_0 w}{e^2\mu_c}} \tag{3}$$

The next step was to investigate the influence of the grating width w on the absorptance of the proposed absorber structure. As shown in Fig. 4**a**, when the width w_2 of the lower grating strip increases from 120 through 135, 150, 165 to 180 nm with fixed $w_1 = 150$ nm, $\mu_{c1} = \mu_{c2} = 0.6$ eV, the corresponding resonant wavelength increases from 11.29 through 12.15, 13.07, 13.57 to 14.46 μm. From Eq. (3) it can be seen that the wavelength of dipole resonance in the graphene strip increases when the grating width w_2 increases, and then the absorption peak exhibits a red shift as w_2 increases. From Eq. (3) it can also be noticed that a larger difference in the width of the bi-layer

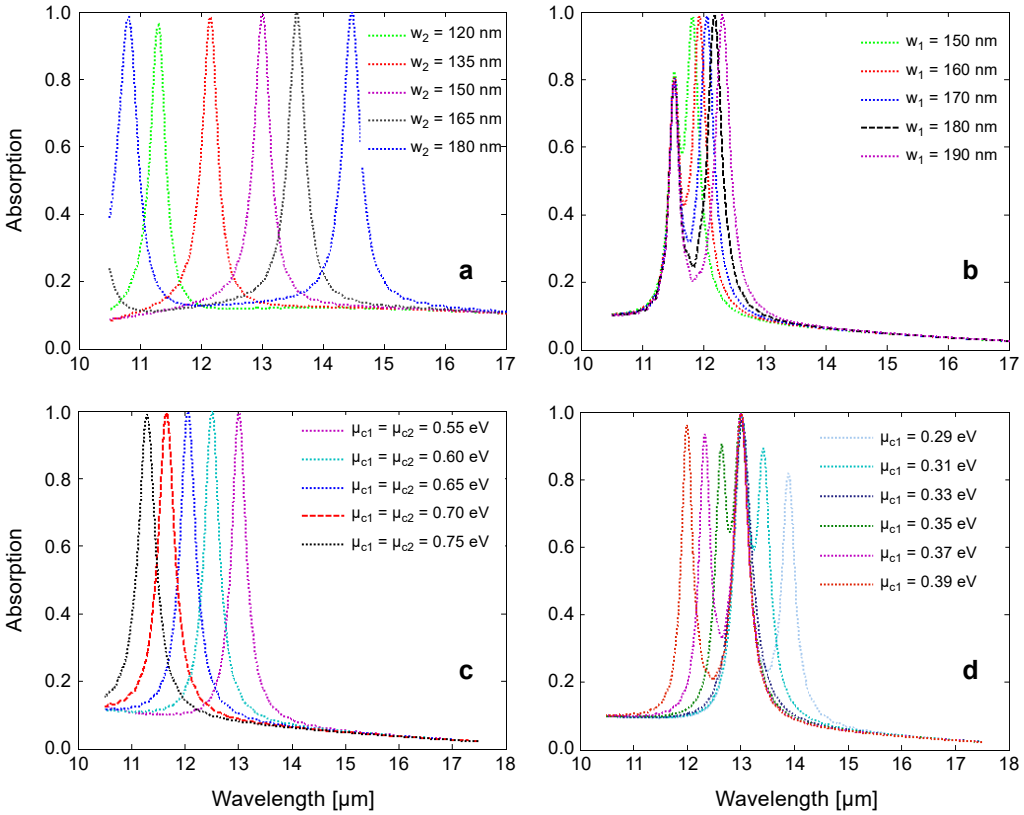

Fig. 4. Absorption spectra with (**a**) different lower graphene grating widths w_2; here $w_1 = 150$ nm and $\mu_{c1} = \mu_{c2} = 0.6$ eV. (**b**) Different upper graphene grating widths w_1; here $w_2 = 80$ nm and $\mu_{c1} = \mu_{c2} = 0.4$ eV. (**c**) $\mu_{c1} = \mu_{c2}$ varying from 0.55 to 0.85 eV. (**d**) $\mu_{c2} = 0.6$ eV, μ_{c1} varying from 0.29 to 0.39 eV.

graphene strip will lead to a larger difference of $|\lambda_1 - \lambda_2|$. The absorption spectra with different upper graphene grating widths w_1 and fixed w_2 = 80 nm, $\mu_{c1} = \mu_{c2}$ = 0.4 eV are shown in Fig. 4**b**. It can be seen that when the width w_2 of the lower grating strip increases from 150 through 160, 170, 180 to 190 nm, the difference in absorption peaks becomes larger. Therefore, the absorption peaks can be tuned by changing the width of the graphene strip. Since the change of chemical potential can vary graphene surface conductivity, therefore the position of the absorption peak can be controlled by chemical potential with the gate voltages technology. It can be seen from Fig. 4**c** that when the chemical potential of the graphene increases from $\mu_{c1} = \mu_{c2}$ = 0.55 eV through 0.6, 0.65, 0.7, 0.75 to 0.8 eV, the corresponding resonant absorption wavelength decreases from 13.58 through 13, 12.49, 12.09, 11.64 to 11.28 μm. This pattern can also be seen in Fig. 4**d**, and from Eq. (3) it can be seen that increasing chemical potential will lead to the decrease in resonance wavelength, therefore, the change in the chemical potential provides another way of tunability.

The next step was to investigate the influence of the grating thickness t_1 on the absorptance of the proposed structure. As shown in Figs. 5**a** and 5**c**, t_1 is increased from

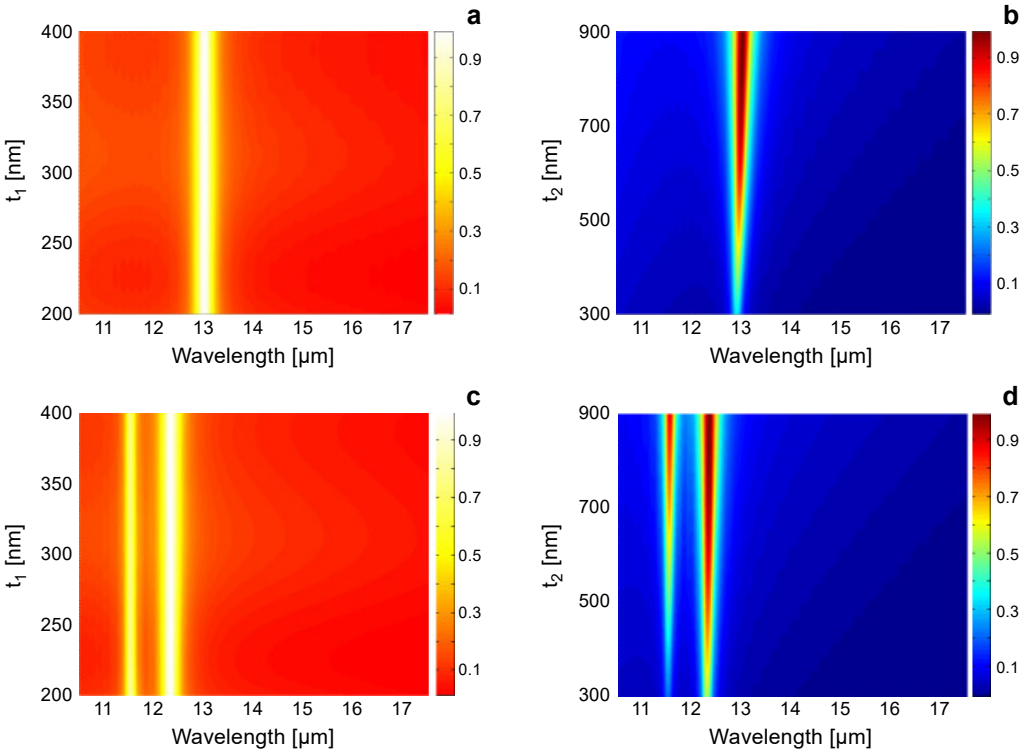

Fig. 5. Absorption spectra with different thickness of SiO_2 grating (t_1) and Al_2O_3 layer (t_2). (**a**, **b**) $w_1 = w_2$ = 150 nm and $\mu_{c1} = \mu_{c2}$ = 0.6 eV. (**c**, **d**) w_1 = 190 nm, w_2 = 80 nm, and $\mu_{c1} = \mu_{c2}$ = 0.4 eV.

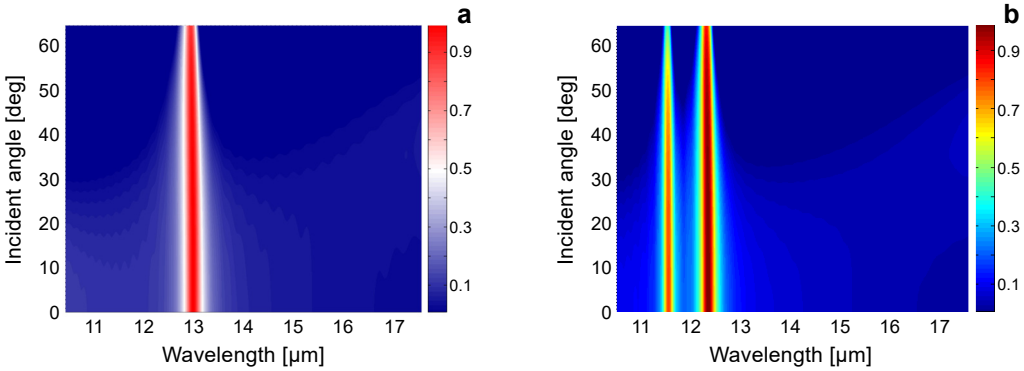

Fig. 6. Absorption as a function of wavelength and the angle of incidence, the angle varying from 5 to 65 deg. (**a**) $w_1 = w_2 = 150$ nm and $\mu_{c1} = \mu_{c2} = 0.6$ eV, (**b**) $w_1 = 190$ nm, $w_2 = 80$ nm, and $\mu_{c1} = \mu_{c2} = 0.4$ eV.

200 to 400 nm, and the spectral position of the absorption peaks is kept unchanged as the thickness increases. For the proposed perfect absorption, most of the input energy is confined in the Al_2O_3 layer. Hence, the thickness t_2 of the Al_2O_3 layer has an effect on the absorption. Figures 5**b** and 5**d** show the absorption spectra with different thickness t_2 of Al_2O_3 layer. It can be seen that when the thickness t_2 of the Al_2O_3 layer increases from 300 to 900 nm, the position of absorption peaks is kept almost unchanged, but the absorption and FWHM increase. This is because the EI of the proposed structure depends on the Al_2O_3 layer. When the thickness of the Al_2O_3 layer is changed from 300 to 900 nm, the EI matching is formed gradually, and then the perfect absorption is achieved. Therefore, the perfect absorption can also be tuned by changing the thickness t_2 of the Al_2O_3 layer.

In practice, the incident electromagnetic wave interacts with the plasmonic absorber with an oblique angle. The absorption spectra as a function of the incident angle are shown in Fig. 6. It can be seen that for a single or double-band absorber, the position of the absorption peak keeps unchanged over a wide angle range of incidence about ±65°. Therefore, the proposed wide-angle single or double-band absorber can be achieved by the graphene strip coupling SiO_2 grating. Moreover, by adding more graphene strips, a multiband perfect absorber can be realized.

3. Conclusions

In conclusion, the absorption characteristics of the graphene strip coupled to SiO_2 grating coated by a Al_2O_3 layer and silver substrate are investigated. Numerical study shows that nearly unity absorption can be achieved in the mid-infrared range by means of EI matching. The position of the absorption peak and the absorptance can be tuned by changing geometrical parameters or chemical potential. Moreover, by controlling the chemical or the graphene width, a double-band perfect absorber can be obtained.

The designed graphene-based absorber has excellent absorption stability over a wide -angle range of incidence around ±65°. The results can be applied in the area of graphene optical filtering, optical switching and slow light in the mid-infrared range.

Acknowledgements – Funding: Supported by National Natural Science Foundation of China (Grant No. 11747091). Supported by the talent and high level thesis cultivation program of School of Physics and Optoelectronics Engineering, Yangtzeu University.

References

[1] NOVOSELOV K.S., GEIM A.K., MOROZOV S.V., JIANG D., ZHANG Y., DUBONOS S.V., GRIGORIEVA I.V., FIRSOV A.A., *Electric field effect in atomically thin carbon films*, Science **306**(5696), 2004, pp. 666–669, DOI: 10.1126/science.1102896.

[2] NOVOSELOV K.S., GEIM A.K., MOROZOV S.V., JIANG D., KATSNELSON M.I., GRIGORIEVA I.V., DUBONOS S.V., FIRSOV A.A., *Two-dimensional gas of massless Dirac fermions in graphene*, Nature **438**, 2005, pp. 197–200, DOI: 10.1038/nature04233.

[3] GRIGORENKO A.N., POLINI M., NOVOSELOV K.S., *Graphene plasmonics*, Nature Photonics **6**, 2012, pp. 749–758, DOI: 10.1038/nphoton.2012.262.

[4] JAMALI A.A., WITZIGMANN B., *Plasmonic perfect absorbers for biosensing applications*, Plasmonics **9**(6), 2014, pp. 1265–1270, DOI: 10.1007/s11468-014-9740-1.

[5] LANDY N.I., SAJUYIGBE S., MOCK J.J., SMITH D.R., PADILLA W.J., *Perfect metamaterial absorber*, Physical Review Letters **100**(20), 2008, article 207402, DOI: 10.1103/PhysRevLett.100.207402.

[6] ZHANG L., WANG Y., ZHOU L., CHEN F., *Tunable perfect absorber based on gold grating including phase-changing material in visible range*, Applied Physics A **125**(5), 2019, article 368, DOI: 10.1007/s00339-019-2669-7.

[7] HE X., YANG J., CHEN D., ZHANG S., HAN Y., ZHANG Z., *Sub-wavenumber linewidth mid-infrared notch filter enabled by a dual-period plasmonic structure*, Optics Communications **428**, 2018, pp. 152–156, DOI: 10.1016/j.optcom.2018.07.066.

[8] GAO Y.X., REN G.B., ZHU B.F., HUANG L., LI H., YIN B., JIANG S.S., *Tunable plasmonic filter based on graphene split-ring*, Plasmonics **11**(1), 2016, pp. 291–296, DOI: 10.1007/s11468-015-0050-z.

[9] XU J.B., HU J.X., WANG R.B., LI Q., LI W.W., GUO Y.F., LIU F.K., ULLAH Z., WEN L., LIU L.W., *Ultra-broadband graphene-InSb heterojunction photodetector*, Applied Physics Letters **111**(5), 2017, article 051106, DOI: 10.1063/1.4997327.

[10] BAQIR M.A., FARMANI A., FATIMA T., RAZA M.R., SHOUKAT S.F., MIR A., *Nanoscale, tunable, and highly sensitive biosensor utilizing hyperbolic metamaterials in the near-infrared range*, Applied Optics **57**(31), 2018, pp. 9447–9454, DOI: 10.1364/AO.57.009447.

[11] SLOVICK B.A., *Negative refractive index induced by percolation in disordered metamaterials*, Physical Review B **95**(9), 2017, article 094202, DOI: 10.1103/PhysRevB.95.094202.

[12] LIU Y.M., ZENTGRAF T., BARTAL G., ZHANG X., *Transformational plasmon optics*, Nano Letters **10**(6), 2010, pp. 1991–1997, DOI: 10.1021/nl1008019.

[13] CHEN F., ZHANG H.F., SUN L.H., LI J.J., YU C.C., *Double-band perfect absorber based on the dielectric grating and Fabry–Perot cavity*, Applied Physics A **125**(11), 2019, article 792, DOI: 10.1007/s00339-019-3101-z.

[14] LU H., GAN X.T., JIA B.H., MAO D., ZHAO J.L., *Tunable high-efficiency light absorption of monolayer graphene via Tamm plasmon polaritons*, Optics Letters **41**(20), 2016, pp. 4743–4746, DOI: 10.1364/OL.41.004743.

[15] LU H., GAN X.T., MAO D., FAN Y.C., YANG D.X., ZHAO J.L., *Nearly perfect absorption of light in monolayer molybdenum disulfide supported by multilayer structures*, Optics Express **25**(18), 2017, pp. 21630–21636, DOI: 10.1364/OE.25.021630.

[16] Li H.J., Ji C.S., Ren Y.Z., Hu J.G., Qin M., Wang L.L., *Investigation of multiband plasmonic metamaterial perfect absorbers based on graphene ribbons by the phase-coupled method*, Carbon **141**, 2019, pp. 481–487, DOI: 10.1016/j.carbon.2018.10.002.
[17] Li H.J., Wang L.L., Zhai X., Scientific Reports **6**, 2016, p. 1.
[18] Chen F., Yao D., Zhang H., Sun L., Yu C., *Tunable plasmonic perfect absorber based on a multilayer graphene strip-grating structure*, Journal of Electronic Materials **48**(9), 2019, pp. 5603–5608, DOI: 10.1007/s11664-019-07422-0.
[19] Cai Y.J., Xu K.D., *Tunable broadband terahertz absorber based on multilayer graphene-sandwiched plasmonic structure*, Optics Express **26**(24), 2018, pp. 31693–31705, DOI: 10.1364/OE.26.031693.
[20] Xiong H., Wu Y.B., Dong J., Tang M.C., Jiang Y.N., Zeng X.P., *Ultra-thin and broadband tunable metamaterial graphene absorber*, Optics Express **26**(2), 2018, pp. 1681–1688, DOI: 10.1364/OE.26.001681.
[21] Xu K.D., Li J.X., Zhang A., Chen Q., *Tunable multi-band terahertz absorber using a single-layer square graphene ring structure with T-shaped graphene strips*, Optics Express **28**(8), 2020, pp. 11482–11492, DOI: 10.1364/OE.390835.
[22] Alharbi R., Irannejad M., Yavuz M., *Au-graphene hybrid plasmonic nanostructure sensor based on intensity shift*, Sensors **17**(1), 2017, article 191, DOI: 10.3390/s17010191.
[23] Jain P., Gupta S., Maiti T., *Simulation and analytical study of optical complex field in nano-corral slits plasmonic lens*, Plasmonics **13**(6), 2018, pp. 2151–2160, DOI: 10.1007/s11468-018-0732-4.
[24] Wen K., Luo X.Q., Chen Z.Y., Zhu W.H., Guo W., Wang X.L., *Enhanced optical transmission assisted near-infrared plasmonic optical filter via hybrid subwavelength structures*, Plasmonics **14**(6), 2019, pp. 1649–1657, DOI: 10.1007/s11468-019-00963-4.
[25] Han X., Wang T., Li X.M., Zhu Y.J., *Dynamically tunable by Kerr effect multichannel filter based on plasmon induced transparencies at optical communication range*, Plasmonics **11**(3), 2016, pp. 729–733, DOI: 10.1007/s11468-015-0102-4.
[26] Chen F., Yao D.Z., Liu Y.N., *Graphene–metal hybrid plasmonic switch*, Applied Physics Express **7**(8), 2014, article 082202, DOI: 10.7567/APEX.7.082202.
[27] Ju L., Geng B.S., Horng J., Girit C., Martin M., Hao Z., Bechtel H.A., Liang X.G., Zettl A., Shen Y.R., Wang F., *Graphene plasmonics for tunable terahertz metamaterials*, Nature Nanotechnology **6**(10), 2011, pp. 630–634, DOI: 10.1038/nnano.2011.146.

Received February 4, 2020
in revised form April 19, 2020